JOURNAL OF MATERIALS SCIENCE 20 (1985) 881–888

The structural degradation and lamellar to rod transition in the Bi–Cd eutectic during unidirectional growth

M. A. SAVAS, R. W. SMITH
Department of Metallurgical Engineering, Queen's University, Kingston, Canada, K7L 3N6

The Bi–Cd eutectic system is a prototype quasi-regular eutectic in which the bismuth-rich phase has a volume fraction of 57%. It shows a high degree of regularity but, clearly, is not a normal (regular) eutectic. Microstructural observations of unidirectionally-grown specimens show that the minor cadmium-rich phase degrades at small temperature gradients and small growth rates. However, the structural refinement resulting from rapid freezing or chemical addition is found to be analogous to that of the F/NF eutectics. A lamellar → rod transition has been achieved at intermediate growth rates by adding 2.0 wt % Sn as a "modifier" to the eutectic alloy. However, this was accompanied by the bismuth phase showing cellular facets of the solid–liquid interface.

Nomenclature

G_L	temperature gradient in the melt ahead of the solid/liquid interface ($^\circ$C cm^{-1})
G_S	temperature gradient in the solid behind the solid–liquid interface ($^\circ$C cm^{-1})
R	growth rate of solid (cm sec^{-1})
S	cooling rate ($^\circ$C sec^{-1}, $^\circ$C h^{-1})
K_S	thermal conductivity in the solid (W m^{-1} K^{-1})
K_L	thermal conductivity in the melt (W m^{-1} K^{-1})
L	latent heat of fusion (J mol^{-1})
ΔT	temperature difference, undercooling ($^\circ$C)
K_1	constant in Equation 2
K_2	constant in Equation 3
D	diffusion coefficient of solute in solid (m^2 sec^{-1})
C	solubility in solid (wt %, at %)
M	molecular weight (g mol^{-1})
ρ	density (g cm^{-3})
γ	interfacial energy, surface tension (J mm^{-2})
R	gas constant, 8.314 J mol^{-1} K^{-1}
r	radius of curvature (μm)
T	temperature (K)
t	time (sec)
F	faceted
NF	non-faceted

1. Introduction

To date, the unidirectional solidification of the Bi–Cd eutectic has received considerable attention because of its low melting point, almost regular morphology and its thermoelectric properties [1–8]. However, no work has been reported on its place as a prototype system of the so-called quasi-regular group anomalous eutectics.

The quasi-regular description was used initially by Miller and Chadwick [9] in order to describe the high degree of regularity in this eutectic. Following the proposals by Hulme and Mullin [10] and Hunt and Hurle [11, 12], Croker *et al.* [5] argued that the unpredicted appearance of an almost regular morphology in the Bi–Cd or any other high volume fraction faceted phase anomalous eutectic arises from the fact that the faceted phase forms the matrix. The structure of such a binary eutectic under the optical microscope may be characterized as an array of sheets and/or fibres of the non-faceted minor phase of various widths in a honeycombe-like matrix of the faceted phase [6].

0022–2461/85 $03.00 + .12

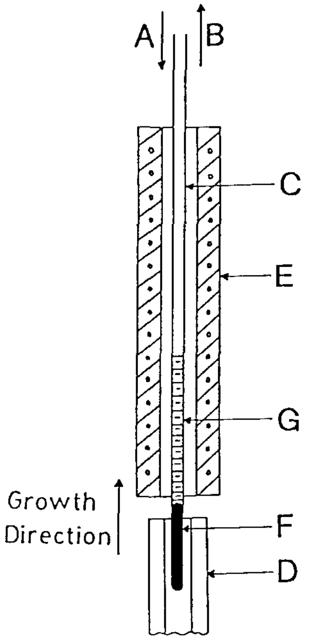

Figure 1 A schematic diagram of the growth apparatus used in this study to solidify the eutectic alloys unidirectionally. A, direction of specimen tube movement; B, connection to drive unit; C, specimen tube; D, cooling device; E, tube furnace; F, solid; G, melt.

The purpose of the present investigation was to establish the influence of the growth conditions on the quasi-regular morphology as well as the structural modification possible by small additions of ternary elements. Before attempting any morphological interpretations a study of the influence of growth conditions was carried out.

2. Experimental details

The eutectic alloys, prepared from 99.9999% pure metals, were grown unidirectionally in a vertical Bridgman-type crystal growth apparatus at controlled growth rates and temperature gradients as described elsewhere [13]. A schematic diagram of the growth apparatus is shown in Fig. 1.

In order to achieve chemical modification, a weighed amount of sodium was added to the molten alloy just before pouring into a small steel mould. In addition, since it was not volatile and also did not attack the specimen tube, tin was used as a modifier and was added while preparing the eutectic alloy.

3. Results and discussion

3.1. Variation of the temperature gradients and the position of the solid–liquid interface during unidirectional growth

The temperature gradients in the liquid (G_L) employed in the present investigation were usually slightly smaller than those used by Hamar and Durand, namely 50° C cm^{-1} [3] and 80° C cm^{-1} [4]. The extent to which the growth rate affected the temperature gradients G_L and G_S at a certain furnace setting and also the position of the solid–liquid interface relative to the furnace were examined. The results are shown collectively in Table I.

TABLE I Experimental data displaying the effects of the furnace setting and the growth rate on temperature gradients

Furnace setting (° C)	Temperature at bottom exit of furnace (° C)	Distance of solid–liquid interface from quench bath at $R \leqslant 10^{-3}$ cm sec^{-1} (cm)	Temperature gradients near the solid–liquid interface (° C cm^{-1})		Growth rate (cm sec^{-1})
			G_L	G_S	
200	122	2.5	9	18	10^{-4}
			9	18	10^{-3}
			4	80	10^{-2}
250	161	0.5	20	20	10^{-4}
			20	20	10^{-3}
			14	20	10^{-2}
350	231	−1.5*	40	38	
			40	38	10^{-4}
			27	42	10^{-3}
500	328	−3.0*	54	54	10^{-4}
			54	54	10^{-3}
			35	–	10^{-2}
600	457	−4.5*	85	85	10^{-4}
			85	85	10^{-3}
			–	–	10^{-2}

*The (—) sign indicates the interface is 4.5 cm below the bottom of the furnace.

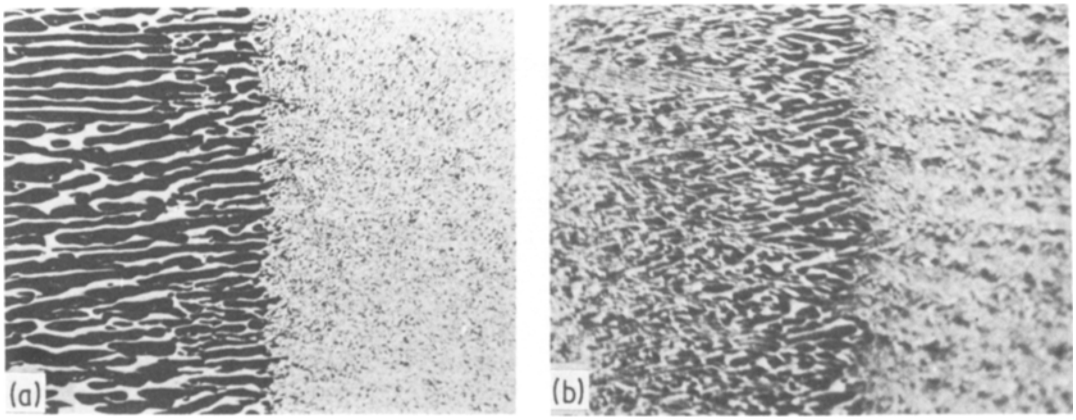

Figure 2 The topography of the solidifcation front and the eutectic morphology behind the solid–liquid interface in Bi–Cd eutectic under different growth rates at a fixed $G_S = 18°\text{C cm}^{-1}$. (a) $R = 1.50 \times 10^{-3}$ cm sec^{-1} (× 190). (b) $R = 5.00 \times 10^{-6}$ cm sec^{-1} (× 95). (Please note that the growth directions are from left to right.)

During unidirectional growth, the temperature gradients G_L and G_S in the vicinity of the solid–liquid interface are related by [14]

$$K_S G_S = K_L G_L + L\rho R \qquad (1)$$

If the container has a lower thermal conductivity than the specimen, then, because this continuity condition must be maintained, the rate of heat removal through the solid controls the rate of movement of the solid–liquid interface and, therefore, the growth rate. Since the distance between the furnace and the quench bath (i.e. water cooling device) was fixed at about 1 cm, increasing the growth rate caused the interface to move closer to the quench bath. This resulted in an increase in G_S and, correspondingly, a relative decrease in G_L to the extent that during normal crystal growth constitutional undercooling arose when $R > 10^{-3}$ cm sec^{-1}.

As has been done in the past [13], the temperature gradients in this work were increased by imposing large temperature differences between the furnace and the quench bath. Once the furnace setting was increased to 350° C or to even higher temperatures the solid–liquid interface moved into the quench bath, even at $R \leqslant 10^{-3}$ cm sec^{-1} (Table I). This rendered the measurement of G_L and G_S problematical.

In addition, the influence of furnace temperature, since it influences G_S and the position of the solid–liquid interface relative to the quench bath, becomes important at small growth rates if the minor eutectic phase has a tendency to degrade during growth.

3.2. The topography of the solid–liquid interface and the relationship of interface undercooling to growth rate

In the Bi–Cd eutectic, the faceted bismuth phase forms the matrix with a volume fraction of 57%. As a result, despite a high entropy of solution value, faceting may not occur during freezing [5]. Small projections and irregularities can be seen at the solid–liquid interface, as shown in Fig. 2a. Nevertheless, there is no evidence that the interface is markedly irregular as may be seen in low volume fraction F/NF eutectics. The eutectic phases can grow in a near-coupled fashion in order to produce the quasi-regular morphology behind the interface [13].

In this study, the relationship of the interface undercooling to the growth rate at a fixed $G_L = 18°\text{ C cm}^{-1}$ was found to be

$$\Delta T R^{-0.46} = \text{constant}\,(K_1). \qquad (2)$$

This implies that the interface undercooling in the Bi–Cd eutectic follows a relationship similar to that derived for normal eutectics, for which it has been proposed that [15, 16]

$$\Delta T R^{-0.5} = \text{constant}\,(K_2). \qquad (3)$$

In anomalous eutectics, a large value of G_L reduces the "lead distance" of one phase relative to the other and so permits sufficient diffusion for coupled growth to take place [17]. Thus, it is to be expected from this argument that G_L will have little influence on eutectics which normally grow with planar solid–liquid interfaces. Only at a low G_L/R value can the planar interface break down into a cellular or cellular–dendritic type. Thus, the Bi–Cd eutectic resembles a normal eutectic. Indeed, microscopic examination shows that G_L alone does not influence the topography of the solid–liquid interface to any noticeable extent. On the other hand, G_S markedly influences the degradation of the cadmium lamellae in the eutectic morphology.

3.3. Structural degradation during growth

The existing theoretical analyses of normal eutectic growth are based entirely on considerations of diffusion in the melt, and assume that diffusion in the solid can be ignored as a factor influencing the phase morphology. Unidirectional growth necessarily imparts a high temperature anneal to the freshly formed fine eutectic phase distribution. In fact, under typical growth conditions unidirectionally grown specimens cool rather slowly. For instance, at $G_S \sim 20^\circ \mathrm{C\,cm^{-1}}$ and $R \sim 10^{-4}\,\mathrm{cm\,sec^{-1}}$, the cooling rate $S = G_S R = 2 \times 10^{-3}\,^\circ \mathrm{C\,sec^{-1}}$ (or $\sim 7.2^\circ \mathrm{C\,h^{-1}}$) is very small. This allows considerable solid-state diffusion in the eutectic structure which permits the as-grown structure to degrade as growth proceeds.

Traditional coarsening laws allow us to analyse the dissolution rate of a "β" particle of radius "r" within an "α"-matrix [18]. Although in the present case geometrical conditions are different and accurate diffusivity, solubility and interfacial energy data are not available, an estimate of the coarsening rate may be made [19]:

$$\frac{\mathrm{d}r}{\mathrm{d}t} = DC\frac{4M_{\mathrm{Cd}}\gamma_{\mathrm{Bi/Cd}} \times 1}{RT\rho_{\mathrm{Cd}}^2 r^2}. \tag{4}$$

For a radius of curvature of 1 μm, the coarsening rate near the eutectic temperature (e.g. ~ 130° C) would be a few tenths of a nanometre per second. This means that within minutes after freezing, the original eutectic morphology may be markedly changed. It is observed that the degradation of cadmium-rich lamellae in the Bi–Cd eutectic becomes most marked at the smallest experimental values of G_S ($18^\circ \mathrm{C\,cm^{-1}}$) combined with the smallest R ($5.00 \times 10^{-6}\,\mathrm{cm\,sec^{-1}}$) since degradation is a function of both the time and temperature. As seen in Fig. 2b, the marked degradation under these conditions starts only about 150 μm from the solid–liquid interface. This corresponds to a lapse of 48 min from the time of freezing. Degradation occurs by the spheroidization and separation of the material at the tips of the cadmium lamellae as reported for the Sn–Cd eutectic [20]. Most of the detached particles adopt circular shapes or cross-sections (Fig. 3a), revealing that the interfacial energy is near isotropic, to minimize their surface energy by minimizing the surface area. As the growth rate is increased progressively, the eutectic morphology exhibits the following sequence of transitions (at $G_S = 18^\circ \mathrm{C\,cm^{-1}}$):

(i) At $R \sim 10^{-4}\,\mathrm{cm\,sec^{-1}}$, degenerate cadmium lamellae are present in the bismuth matrix (Fig. 3b).

(ii) The characteristic quasi-regular morphology becomes apparent when the growth rate is increased to $R \sim 10^{-3}\,\mathrm{cm\,sec^{-1}}$ (Fig. 3c).

(iii) The G_L/R ratio is low enough to produce sufficient constitutional undercooling for the growth of plate-like cadmium primaries when $R \geqslant 2.65 \times 10^{-2}\,\mathrm{cm\,sec^{-1}}$, (Fig. 3d).

At a fixed growth rate, larger G_S values reduce the rate of degradation of the cadmium lamellae. It is also noteworthy that the extent of degradation is also a function of the position of the solid–liquid interface which is, like G_S, partly determined by the initial furnace setting. As shown in Table I, when the furnace setting is at 200° C, i.e. $G_S = 18^\circ \mathrm{C\,cm^{-1}}$, and at growth rates $R \leqslant 10^{-3}\,\mathrm{cm\,sec^{-1}}$, the interface moves into the furnace. In this case, the freshly formed eutectic material behind the interface is only slightly below the eutectic temperature. To make things worse, at small growth rates the solid eutectic has to be exposed to this hot zone for a longer period of time. This allows sufficient time for extensive solid-state diffusion. The interface does not move into the furnace at furnace settings greater than 250° C and so no marked degradation occurs.

In passing, it may be noted that the anisotropy of the interfacial energy is a factor which, in general, stabilizes the eutectic morphology [21]. It may be due to this fact that degradation and spheroidization in low volume fraction faceted phase anomalous eutectics is not often reported in the literature.

3.4. Lamellar to rod transition: modification of the cadmium phase

In essence the Bi–Cd eutectic and other quasi-regular eutectics can be treated as normal eutectics when "modification" is considered, because the minor eutectic phase to be modified in this case is the non-faceted one, not the faceted matrix. At

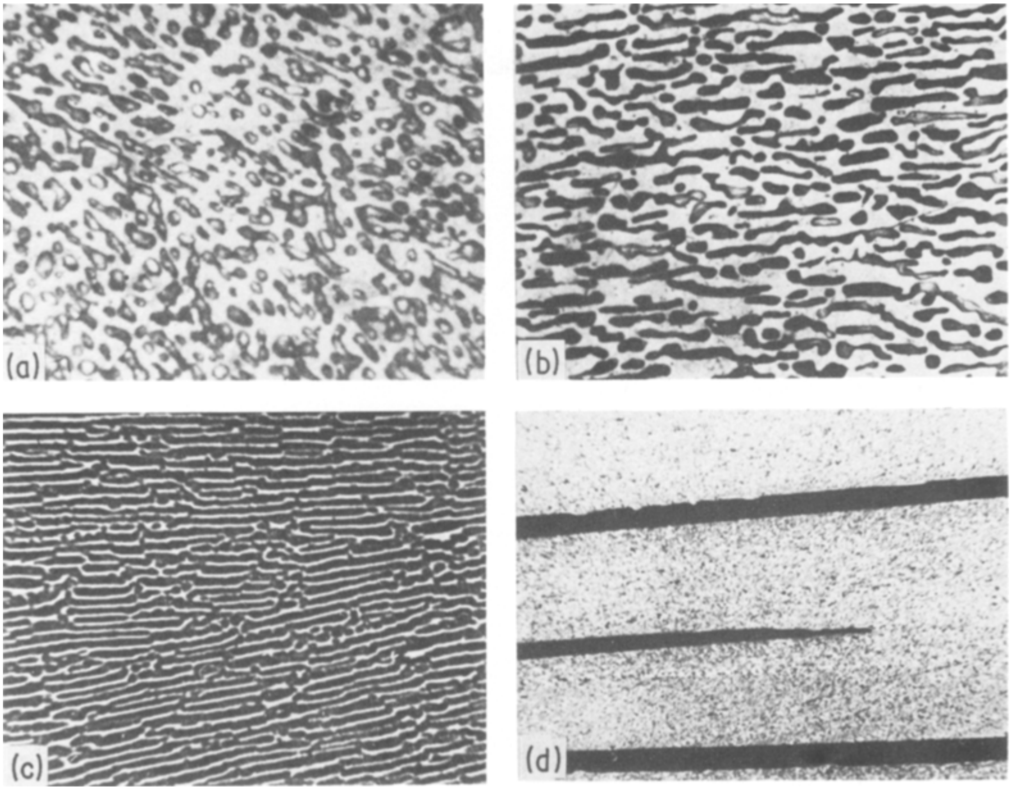

Figure 3 The sequence of transitions in the morphology of the cadmium phase of Bi–Cd eutectic with increased growth rates at a fixed $G_S = 18° \text{C cm}^{-1}$. (a) Markedly degraded and spheroidized cadmium phase, $R = 5.00 \times 10^{-6}$ cm sec^{-1} (× 1080). (b) Degenerate cadmium lamellae, $R = 2.0 \times 10^{-4}$ cm sec^{-1} (× 415). (c) Characteristic quasi-regular cadmium morphology, $R = 2.50 \times 10^{-3}$ cm sec^{-1} (× 200). (d) Plate-like cadmium primaries present within the disturbed eutectic morphology, $R = 2.65 \times 10^{-2}$ cm sec^{-1}, $G_S = 80° \text{C cm}^{-1}$ (× 54).

present, the mechanism of the modification of low volume fraction anomalous eutectics is well understood [22–24], i.e. by the strong adsorption of the alkali metals or alkaline-earths on the high entropy of solution phase during growth. No quantitative theory of modification has been formulated yet which can predict that a given impurity will cause a lamellar → rod transition in a given normal eutectic. In this study, following Tiller's proposal [25] it was presumed that to the extent that any effective modifying element can be found for the cadmium phase of the Bi–Cd eutectic, then tin would appear to be a promising one.

So far, two proposals have been put forward to account for the lamellar → rod transition. According to the impurity (solute) segregation approach [26], when the distribution coefficients of particular impurity in the eutectic phases are very different, the lamellae of one phase grow into the melt ahead of those of the other, and the lamellae of the lagging phase (i.e. the constitutionally undercooled phase) then break up into cells separated by the other phase, which would be an alternative way of describing a rod structure. However, it has been argued that there appears to be both theoretical and experimental evidence against the solute segregation approach [27, 28]. In all lamellar → rod transitions the evidence is that such a transition is likely to occur when the solid–liquid interface becomes curved (cellular) for any reason [27], i.e. when the departure from the preferred low energy lamellar plane becomes sufficiently large, then the rod-like growth becomes energetically favourable. During the unidirectional growth of Bi–Cd eutectic, the tin impurity is rejected by both sets of lamellae, slightly more by cadmium than bismuth. This build-up of tin causes considerable undercooling and a cellular solid–liquid interface can be stabilized.

In this part of the present study the tin content

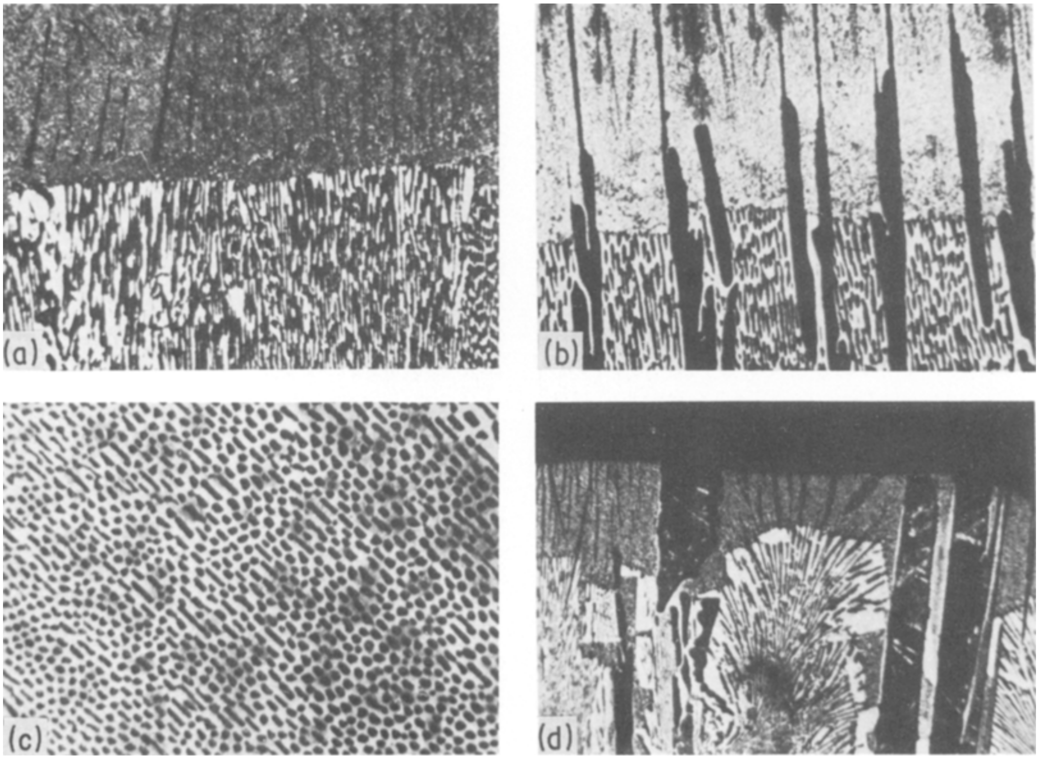

Figure 4 The sequence of transitions observed at the solid–liquid interface of the Bi–Cd eutectic after 2.0 wt% tin addition. (a) $R = 10^{-4}$ cm sec^{-1}, $G_L = 35°$ C cm^{-1}. Cubic (or fish spine) cells (X 100). (b) $R = 10^{-3}$ cm sec^{-1}, $G_L = 35°$ C cm^{-1}. Cubic cells (X 100). (c) $R = 10^{-3}$ cm sec^{-1}, $G_L = 35°$ C cm^{-1}. Transverse section (X 200). (d) $R = 10^{-3}$ cm sec^{-1}, $G_L = 26°$ C cm^{-1}. Cubic cells and trigonal cells (X 100). (Please note that the growth directions are from bottom to top in Figs. 4a, b and d.)

and furnace temperature were kept constant at 2.0 wt% and 325° C, respectively, with the growth rate being varied from 10^{-5} cm sec^{-1} to 10^{-2} cm sec^{-1}. (Please note that since G_L was dependent on the growth rate it dropped from 35 to 26° C cm^{-1} when the growth rate was increased from 10^{-5} to 10^{-2} cm sec^{-1}). Under those conditions, a progressive increase of the growth rate influenced the eutectic morphology as follows:

(i) At small growth rates, i.e. 10^{-5} and 10^{-4} cm sec^{-1}, the constitutional undercooling developed ahead of the solid–liquid interface is small and so is the depth to which a cell can grow into the melt (Fig. 4a). As compared with the pure (i.e. unmodified) eutectic alloy, the solid–liquid interface is planar within each very flat and wide cell which was previously called a fish spine cell or a cubic cell [29].

(ii) With an increase in growth rate the constitutional undercooling is increased and very definite cubic cells are stabilized at around 10^{-3} cm sec^{-1} (Fig. 4b). Moreover, the cadmium dendrites start to grow at the cell boundaries where the tin build-up and therefore the constitutional undercooling should be the largest along the solid–liquid interface. In this case, a fully rod-like cadmium morphology can be identified in the solidified alloy (Figs. 4b and c).

(iii) As the growth rate is increased even further, to 10^{-2} cm sec^{-1}, both trigonal cells and cubic cells are formed at the solid–liquid interface and the rod-like cadmium morphology is replaced by a truly cellular morphology (Fig. 4d).

During the lamellar → rod transition a penalty is incurred by the system. Since the low energy habit is lost at the solid–liquid interface during the cellular growth the cadmium phase should be very susceptible to degradation. Indeed, the cadmium phase coarsens extensively near the cell and grain boundaries, as shown in Figs. 5a and b. (Large tin concentrations would produce a solid which has a lower melting point than the eutectic phases and

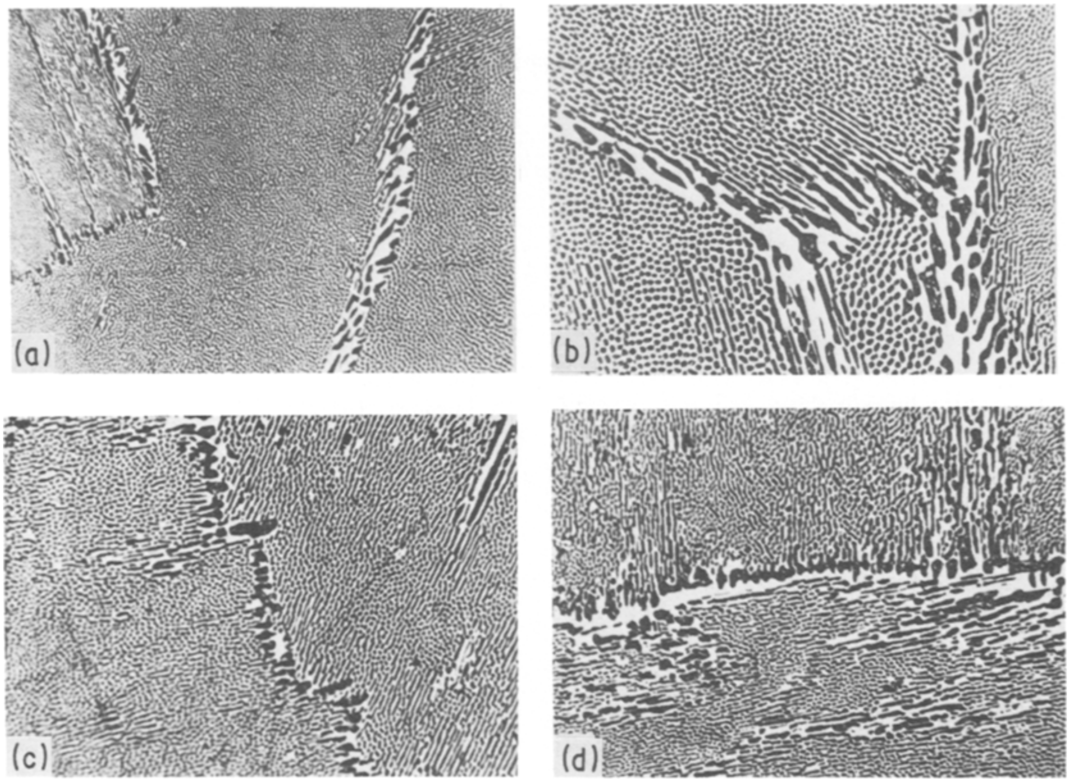

Figure 5 Degradation and coarsening behaviour of the cadmium phase in the 2.0 wt % tin modified Bi–Cd eutectic. $G_S = 35° C cm^{-1}$ ($G_L = 40° C cm^{-1}$), $R = 4.60 \times 10^{-4}$ cm sec^{-1}). (a) Variations of coarsening behaviour in the vicinity of cell and grain boundaries (× 100). (b) A closer view of the coarsened cadmium phase at the cell boundaries (× 200). (c) and (d) Coarsened cadmium phase along the grain boundary (× 100).

so coarsening in these regions might be aggravated by interfacial melting.) Depending on the alignment of the cadmium phase and with a relatively large tin concentration, two sorts of coarsening behaviour are observed in the vicinity of a boundary:

(a) A larger cadmium particle near a boundary coarsens at the expense of the smaller ones in the adjacent grain to form a single large particle across the boundary (Fig. 5c).

(b) The cadmium particles in a grain may agglomerate and form a continuous phase running parallel to the boundary (Fig. 5d).

Large growth rates and chill casting both refine and disturb the cadmium lamellae without promoting a rod transition. Sodium and tin additions to the chill-cast specimens further refine the cadmium lamellae. As expected, the tendency to become rod-like seems more evident in the bismuth-rich off-eutectic alloys. The morphology in this condition is similar to the Sb–Cu_2Sb eutectic morphology in which the volume fraction of the antimony faceted phase is almost 60% [13].

4. Conclusions

1. Any interpretations as to the growth mode of the Bi–Cd eutectic must be made with due caution. A small G_S combined with a small R value induce the degradation and coarsening of the cadmium phase. At a small value of G_S, 18° C cm^{-1}, the relationship of the morphology of the phase to the growth rate may be reported as follows:

Complete degradation ($R \leqslant 10^{-5}$ cm sec^{-1}) →

Degenerate lamellar ($R \sim 10^{-4}$ cm sec^{-1}) →

Quasi-regular ($R \sim 10^{-3}$ cm sec^{-1}) →

Disturbed quasi-regular plus plate-like cadmium primaries ($R \geqslant 2.65 \times 10^{-2}$ cm sec^{-1}).

Hence, the characteristic quasi-regular morphology can be seen only at intermediate growth rates.

2. It appears that the degenerate lamellar cadmium morphology in the Bi–Cd eutectic does not arise directly during growth, but is actually a partially degraded solidification structure.

3. The modification behaviour of anomalous eutectics is determined, in part, by the volume fraction. Once the volume fraction of the faceted eutectic phase exceeds 50% it becomes the matrix. Then, to achieve a structural change the minor non-faceted eutectic phase is modified, but not the faceted matrix. To this end, the cadmium phase of the Bi–Cd eutectic alloy is transformed from a lamellar to a rod morphology at some intermediate growth rates in the presence of 2.0 wt% tin as a modifier.

Acknowledgements

This study is part of a general investigation of phase transformation which has been in progress in the laboratory of RWS for many years. Financial support has been received from many sources but particularly from the National Science and Engineering Research Council of Canada (and its predecessor, the National Research Council) and from Queen's University. MAS has been in receipt of a R. S. McLaughlin Fellowship. All support is gratefully acknowledged.

References

1. L. V. DAVIES, *J. Austral. Inst. Metals* **10** (1965) 282.
2. E. P. WHELAN and C. W. HAWORTH, *ibid.* **12** (1967) 77.
3. R. HAMAR and F. DURAND, *Mem. Sci. Rev. Met.* **69** (1972) 143.
4. *Idem, ibid.* **69** (1972) 151.
5. M. N. CROKER, R. S. FIDLER and R. W. SMITH, *Proc. Roy. Soc.* **A335** (1973) 15.
6. *Idem, J. Cryst. Growth* **30** (1975) 198.
7. F. S. GALASSO, F. C. DOUGLAS and J. A. BATT, *J. Metals* **22** (1970) 40.
8. I. H. MOON, Y. L. KIM and I. S. AHN, *J. Mater. Sci.* **16** (1981) 1367.
9. W. A. MILLER and G. A. CHADWICK, in "The Solidification of Metals" (ISI, London, 1968) p. 49.
10. K. F. HULME and J. B. MULLIN, *Solid State Electronics* **5** (1962) 211.
11. J. D. HUNT and D. T. J. HURLE, *Trans. Met. Soc. AIME* **242** (1968) 1043.
12. *Idem,* in "The Solidification of Metals" (ISI, London, 1978) p. 182.
13. M. A. SAVAS and R. W. SMITH, *J. Crystal Growth* in press.
14. W. C. WINEGARD, "An Introduction to the Solidification of Metals", Institute of Metals Monograph and Report Series No. 29 (Institute of Metals, London, 1964).
15. J. D. HUNT and K. A. JACKSON, *Trans. Met. Soc. AIME* **236** (1966) 1129.
16. R. M. JORDAN and J. D. HUNT, *Met. Trans.* **3** (1972) 1385.
17. J. J. FAVIER and M. TURPIN, *Acta Metall.* **27** (1979) 1021.
18. F. GREENWOOD, *ibid.* **4** (1956) 243.
19. C. LEMAIGNAN, *ibid.* **29** (1981) 1379.
20. D. R. H. JONES, *J. Crystal Growth* **22** (1974) 34.
21. J. VAN SUCHTELEN, *ibid.* **43** (1978) 28.
22. C. B. KIM and R. W. HEINE, *J. Inst. Metals.* **92** (1963–64) 367.
23. H. FREDERIKSON, M. HILLERT and N. LANGE, *ibid.* **101** (1973) 285.
24. D. L. BARAGAR, M. SAHOO and R. W. SMITH, *J. Crystal Growth* **41** (1977) 278.
25. W. A. TILLER, *Acta Metall.* **5** (1957) 56.
26. G. A. CHADWICK, *J. Inst. Metals* **91** (1962–63) 298.
27. J. D. HUNT and J. P. CHILTON, *ibid.* **91** (1962–63) 338.
28. J. D. HUNT, *ibid.* **94** (1966) 125.
29. D. L. BARAGAR, M. SAHOO and R. W. SMITH, in Proceedings of the International Conference on Solidification and Casting, Sheffield, UK (1977) p. 88.

Received 6 April
and accepted 10 May 1984